PERGAMON

International Journal of Solids and Structures 38 (2001) 3945–3963

INTERNATIONAL JOURNAL OF SOLIDS and STRUCTURES

www.elsevier.com/locate/ijsolstr

Limit analysis of orthotropic structures based on Hill's yield condition

Antonio Capsoni, Leone Corradi *, Pasquale Vena

Department of Structural Engineering, Politecnico di Milano, Piazza Leonardo da Vinci 32, I-20133 Milano, Italy

Received 6 October 1999; in revised form 22 May 2000

Abstract

The limit analysis problem, which permits the direct computation of the limit load of rigid-perfectly plastic solids and structures, is considered with reference to anisotropic materials. As a starting step, attention is focused on Hill's orthotropic condition, for which an explicit expression of the dissipation power in terms of strain rates is established. On this basis, numerical procedures successfully employed in the isotropic (von Mises') case can be used in this context, as some examples illustrate. © 2001 Elsevier Science Ltd. All rights reserved.

Keywords: Plasticity; Orthotropy; Limit analysis

1. Introduction

Limit analysis is the branch of plasticity that predicts the load bearing capacity of ductile structures without resorting to evolutive elastic–plastic computations. As soon as the fundamental theorems were established, connections with mathematical programming theory were recognized (Charnes and Greenberg, 1951) and early attempts toward the direct computation of limit loads rested on the use of linear (see Cohn and Maier, 1979 for a summary of results) and non-linear (e.g., Belytschko and Hodge, 1970; Bottero et al., 1980; Casciaro and Cascini, 1982) programming algorithms. However, the computational burden required by the solution of meaningful problems was significant and the parallel development of efficient algorithms for finite element elastic–plastic analysis eventually diverted the attention of researchers from direct methods.

In recent years, a revival of interest on limit analysis has been observed (Yang, 1988; Liu et al., 1995; Sloan and Kleeman, 1995; Jiang, 1995; Capsoni and Corradi, 1997; Ponter and Carter, 1997), mainly exploiting the kinematic (upper bound) theorem and referring to the von Mises' yield criterion. In this context, the problem reduces to the search of the minimum of a convex, albeit non-smooth functional. The formulation itself was proposed about thirty years ago (see Hodge and Belytschko, 1968 for plates in bending), but the developments occurred since then both in finite element modeling and in solution

* Corresponding author. Tel.: +39-02-2399, ext. 4224; fax: +39-02-2399-4220.
E-mail address: corradi@stru.polimi.it (L. Corradi).

PII: S0020-7683(00)00241-9

algorithms permit nowadays a far better computational efficiency. Problems involving up to 40 000 plane elements, with automatically designed and refined meshes, were effectively solved (Christiansen and Andersen, 1999; Christiansen and Pedersen, 1999), showing that direct methods are no doubt competitive with the search of the limit load by means of elastic–plastic computations up to collapse.

The kinematic theorem of limit analysis brings the search of the limit load to a minimum problem. The functional to be minimized is the power dissipated by the solid in the motion corresponding to a *mechanism*. For any convex yield criterion, the *power of dissipation* per unit volume is a uniquely defined function of strain rates and its value can be computed on the basis of Hill's maximum principle (Koiter, 1960). However, the efficiency of most limit analysis algorithms demands that the dissipation power be explicitly expressed in terms of strain rates and these expressions are only available for a limited number of *isotropic* yield conditions, such as von Mises' and Drucker-Prager's. On the other hand, the strength properties of some important engineering materials do show anisotropy and the extension of limit analysis methods to this context, a virtually unexplored field, seems worth investigating.

As a first step in this direction, this paper considers the yield condition proposed by Hill (1947), a relatively simple extension of von Mises' criterion that can account for orthotropic yielding. A method for constructing the expression of the relevant dissipation power starting from the known expression for the isotropic (von Mises') case is proposed. This is the only information required to apply to orthotropic problems limit analysis methods successfully employed within the framework of isotropy.

A few examples illustrate the results and assess their validity. They also underline some inherent limitations of Hill's criterion, which imposes rather severe constraints on the uniaxial yield limits in the orthotropy directions. In fact, the criterion is unable to accurately represent the mechanical behavior of several materials of engineering interest, such as fiber reinforced composites. However, it is felt that the results presented can be regarded as an useful starting step and extensions to more realistic anisotropic yield functions (such as the Tsai and Wu, 1971, criterion) can be foreseen.

2. The rigid-perfectly plastic model

Limit analysis deals with rigid-perfectly plastic materials. Such a constitutive model assumes that stresses are confined within a *convex* domain, which, in this paper, is defined by the inequality

$$\varphi(\boldsymbol{\sigma}) = f(\boldsymbol{\sigma}) - \sigma_0 \leqslant 0 \qquad f = \sqrt{\frac{1}{2}\boldsymbol{\sigma}^{\mathrm{t}}\mathbf{P}\boldsymbol{\sigma}} \tag{1a, b}$$

φ is the yield function (regular for simplicity), σ_0 a suitable yield limit and $\mathbf{P}$ a symmetric, positive definite or semidefinite, matrix. Deformations cannot occur if $\varphi < 0$, while plastic flow may develop when Eq. (1a) holds as equality. In this case, strain rates obey the *normality rule*

$$\varphi = 0: \quad \dot{\varepsilon} = \left\{\frac{\partial \varphi}{\partial \boldsymbol{\sigma}}\right\}\dot{\lambda} = \left\{\frac{\partial f}{\partial \boldsymbol{\sigma}}\right\}\dot{\lambda} = \frac{\dot{\lambda}}{2\sigma_0}\mathbf{P}\boldsymbol{\sigma}, \quad \dot{\lambda} \geqslant 0. \tag{2}$$

When writing Eq. (2), account was taken of the expression Eq. (1b) of the *effective stress* $f(\boldsymbol{\sigma})$ and of the fact that $f = \sigma_0$ when plastic flow develops. The column vectors

$$\boldsymbol{\sigma} = \{\, \sigma_x \quad \sigma_y \quad \sigma_z \quad \tau_{xy} \quad \tau_{yz} \quad \tau_{zx} \,\}^{\mathrm{t}} \quad \dot{\boldsymbol{\varepsilon}} = \{\, \dot{\varepsilon}_x \quad \dot{\varepsilon}_y \quad \dot{\varepsilon}_z \quad \dot{\gamma}_{xy} \quad \dot{\gamma}_{yz} \quad \dot{\gamma}_{zx} \,\}^{\mathrm{t}} \tag{3}$$

represent stresses and strain rates. Note that for shear strains, the engineering definitions, twice the corresponding tensorial components, are adopted.

The limit analysis problem considers a rigid-perfectly plastic solid subject to body forces $k\mathbf{F}$ on its volume Ω and surface tractions $k\mathbf{f}$ on the free portion $\partial_{\mathrm{F}}\Omega$ of its boundary. The constrained boundary $\partial_{\mathrm{U}}\Omega$

is fixed. Loads are defined as *basic values* $\mathbf{F}$ and $\mathbf{f}$, affected by a load multiplier k, and the value s of k for which collapse is attained (*collapse multiplier*) is sought.

The *kinematic theorem* of limit analysis states that s is the optimal value of the minimum problem

$$s = \min_{\dot{\varepsilon},\dot{\mathbf{u}}} \int_{\Omega} \hat{D}(\dot{\boldsymbol{\varepsilon}})\,\mathrm{d}\mathbf{x}, \tag{4a}$$

$$\text{subject to} \quad \dot{\boldsymbol{\varepsilon}} = \nabla_{\mathrm{S}}\dot{\mathbf{u}} \quad \text{in } \Omega \qquad \dot{\mathbf{u}} = \mathbf{0} \quad \text{on } \partial_{\mathrm{U}}\Omega, \tag{4b}$$

$$\dot{\boldsymbol{\varepsilon}} \in \mathsf{D}_{\varepsilon} \quad \text{in } \Omega, \tag{4c}$$

$$\Pi(\dot{\mathbf{u}}) = \int_{\Omega} \mathbf{F}^{\mathrm{t}}\dot{\mathbf{u}}\,\mathrm{d}\mathbf{x} + \int_{\partial_{\mathrm{F}}\Omega} \mathbf{f}^{\mathrm{t}}\dot{\mathbf{u}}\,\mathrm{d}\mathbf{x} = 1. \tag{4d}$$

In Eq. (4a), $\hat{D}(\dot{\varepsilon})$ is the *dissipation power* per unit volume. Eq. (4b) express compatibility, associating to a velocity field $\dot{\mathbf{u}}$, vanishing on the constrained boundary, the consequent strain rate distribution ($\nabla_{\mathrm{S}}\dot{\mathbf{u}}$ is the symmetric part of the velocity gradient). Eq. (4c) establishes the *plastically admissible* nature of strain rates, confining them within the (convex) domain D_{ε}, the subspace spanned by the outward normals to the yield function. This condition enforces consistency with the constitutive model, in that strain rates obey the normality rule Eq. (2), and together with Eq. (4b) defines a *mechanism*. $\Pi(\dot{\mathbf{u}})$ denotes the power of basic loads, which Eq. (4d) normalizes to unity.

The dissipation power is expressed by Hill's maximum principle as

$$\hat{D}(\dot{\boldsymbol{\varepsilon}}) = \max_{\sigma} \boldsymbol{\sigma}^{\mathrm{t}}\dot{\boldsymbol{\varepsilon}} \quad \text{subject to} \quad \varphi(\boldsymbol{\sigma}) \leqslant 0. \tag{5}$$

The value $\boldsymbol{\sigma}_{(\varepsilon)}$ of $\boldsymbol{\sigma}$ solving the problem Eq. (5) is a stress state associated to $\dot{\varepsilon}$ through the normality rule, uniquely defined if the domain $\varphi(\boldsymbol{\sigma}) \leqslant 0$ is strictly convex. When the domain is convex but not strictly so, $\boldsymbol{\sigma}_{(\varepsilon)}$ may not be unique, but the power of dissipation is still a uniquely defined function of strain rates, which can be written as $\hat{D} = \boldsymbol{\sigma}^{\mathrm{t}}_{(\varepsilon)}\dot{\boldsymbol{\varepsilon}}$. By virtue of Eq. (2) and since $f(\sigma_{(\varepsilon)}) = \boldsymbol{\sigma}_0$, its expression becomes

$$\hat{D} = \boldsymbol{\sigma}^{\mathrm{t}}_{(\varepsilon)}\dot{\boldsymbol{\varepsilon}} = \boldsymbol{\sigma}^{\mathrm{t}}_{(\varepsilon)}\left\{\frac{\partial f}{\partial \boldsymbol{\sigma}}\right\}_{\boldsymbol{\sigma}_{(\varepsilon)}} \qquad \dot{\lambda} = f\left(\boldsymbol{\sigma}_{(\varepsilon)}\right)\dot{\lambda} = \sigma_0\dot{\lambda}. \tag{6}$$

Use was made of the relation $f(\boldsymbol{\sigma}) = \boldsymbol{\sigma}^{\mathrm{t}}\{\partial f/\partial\boldsymbol{\sigma}\}$, a consequence of the homogeneous of degree one nature of function $f(\boldsymbol{\sigma})$.

An explicit expression of the dissipation power in terms of strain rates requires the definition of the corresponding expression $\dot{\lambda} = \dot{\lambda}(\dot{\boldsymbol{\varepsilon}})$. To this purpose, note that the normality rule Eq. (2) implies

$$\dot{\boldsymbol{\varepsilon}}^{\mathrm{t}}\boldsymbol{\Theta}\dot{\boldsymbol{\varepsilon}} = \frac{\dot{\lambda}^2}{4\sigma_0^2}\boldsymbol{\sigma}^{\mathrm{t}}\mathbf{P}\boldsymbol{\Theta}\mathbf{P}\boldsymbol{\sigma} \tag{7}$$

for any (symmetric) matrix $\boldsymbol{\Theta}$. If one of such matrices can be found satisfying the condition

$$\boldsymbol{\sigma}^{\mathrm{t}}\mathbf{P}\boldsymbol{\Theta}\mathbf{P}\boldsymbol{\sigma} = 4\sigma_0^2 \quad \forall\boldsymbol{\sigma} \text{ such that } \varphi(\boldsymbol{\sigma}) = 0 \tag{8}$$

one obtains

$$\dot{\lambda} = \sqrt{\dot{\boldsymbol{\varepsilon}}^{\mathrm{t}}\boldsymbol{\Theta}\dot{\boldsymbol{\varepsilon}}}. \tag{9}$$

On the other hand, $\varphi(\boldsymbol{\sigma}) = 0$ implies $\boldsymbol{\sigma}^{\mathrm{t}}\mathbf{P}\boldsymbol{\sigma} = 2\sigma_0^2$. Hence any matrix Θ such that

$$\mathbf{P}\boldsymbol{\Theta}\mathbf{P} = 2\mathbf{P} \tag{10}$$

represents a legitimate expression. If matrix **P** is non-singular, Eq. (10) implies

$$\boldsymbol{\Theta} = 2\mathbf{P}^{-1}. \tag{11}$$

When **P** is merely positive semidefinite, the normality rule establishes some constraints among the components of $\dot{\boldsymbol{\varepsilon}}$. In this case, more than one matrix Θ can be defined consistently with Eq. (10). Each of them provides the same expression for $\dot{\lambda}$ if the constraints on strain rates are accounted for.

As an example, consider von Mises' yield condition. The relevant effective stress is expressed by Eq. (1b), with

$$\mathbf{P}^{\mathrm{I}} = \begin{bmatrix} 2 & -1 & -1 & 0 & 0 & 0 \\ -1 & 2 & -1 & 0 & 0 & 0 \\ -1 & -1 & 2 & 0 & 0 & 0 \\ - & - & - & - & - & - \\ 0 & 0 & 0 & 6 & 0 & 0 \\ 0 & 0 & 0 & 0 & 6 & 0 \\ 0 & 0 & 0 & 0 & 0 & 6 \end{bmatrix}, \tag{12}$$

where superscript I was introduced to underline that the condition applies to isotropic behavior. The rank deficiency of matrix $\mathbf{P}^{\mathrm{I}}$ indicates the presence of a constraint on $\dot{\boldsymbol{\varepsilon}}$, which is easily identified with the incompressibility condition

$$\dot{\varepsilon}_x + \dot{\varepsilon}_y + \dot{\varepsilon}_z = 0 \tag{13}$$

i.e., the plastically admissible domain D_{ε} for strain rates is the deviatoric subspace.

It can be verified by direct substitution that (among others) both the following matrices comply with Eq. (10):

$$\boldsymbol{\Theta}_1^{\mathrm{I}} = \frac{2}{9}\begin{bmatrix} 2 & -1 & -1 & 0 & 0 & 0 \\ -1 & 2 & -1 & 0 & 0 & 0 \\ -1 & -1 & 2 & 0 & 0 & 0 \\ - & - & - & - & - & - \\ 0 & 0 & 0 & 3/2 & 0 & 0 \\ 0 & 0 & 0 & 0 & 3/2 & 0 \\ 0 & 0 & 0 & 0 & 0 & 3/2 \end{bmatrix} \quad \boldsymbol{\Theta}_2^{\mathrm{I}} = \frac{1}{3}\begin{bmatrix} 2 & 0 & 0 & 0 & 0 & 0 \\ 0 & 2 & 0 & 0 & 0 & 0 \\ 0 & 0 & 2 & 0 & 0 & 0 \\ - & - & - & - & - & - \\ 0 & 0 & 0 & 1 & 0 & 0 \\ 0 & 0 & 0 & 0 & 1 & 0 \\ 0 & 0 & 0 & 0 & 0 & 1 \end{bmatrix}. \tag{14a, b}$$

The two apparently different expressions for $\dot{\lambda}$ obtained on this basis from Eq. (9) actually coincide if one of the strain rate components is eliminated by using Eq. (13).

3. Hills orthotropic condition and relevant dissipation power

A relatively simple yield function accounting for orthotropic yielding was proposed by Hill (1947) as an extension of the von Mises' criterion. If the coordinate axes (x, y, z) are identified with the axes of orthotropy, its expression reads

$$\varphi(\boldsymbol{\sigma}) = \frac{1}{\sqrt{2}}\left[\alpha_{xy}(\sigma_x - \sigma_y)^2 + \alpha_{yz}(\sigma_y - \sigma_z)^2 + \alpha_{zx}(\sigma_z - \sigma_x)^2 + 6\eta_{xy}\tau_{xy}^2 + 6\eta_{yz}\tau_{yz}^2 + 6\eta_{zx}\tau_{zx}^2\right]^{1/2} - \sigma_0 \leqslant 0, \tag{15}$$

where σ_0 is a reference yield stress. $\alpha_{k\ell}$ and $\eta_{k\ell}$ are dimensionless material constants, expressed as functions of the uniaxial yield stresses $\bar{\sigma}_k$ in the three orthotropy directions and of the shear yield stresses $\bar{\tau}_{k\ell}$ by the relations

$$\alpha_{k\ell} = \frac{\sigma_0^2}{\bar{\sigma}_k^2} + \frac{\sigma_0^2}{\bar{\sigma}_\ell^2} - \frac{\sigma_0^2}{\bar{\sigma}_m^2} \qquad \eta_{k\ell} = \frac{1}{3}\frac{\sigma_0^2}{\bar{\tau}_{k\ell}^2} \quad (k,\ell,m = x,y,z). \tag{16a, b}$$

The admissible stress domain $\varphi(\sigma) \leqslant 0$ is convex if all these constants are non-negative, a requirement that introduces rather severe restrictions among the values of $\bar{\sigma}_k$. The effective stress f is given by Eq. (1b), with

$$\mathbf{P} = \begin{bmatrix} \alpha_{zx}+\alpha_{xy} & -\alpha_{xy} & -\alpha_{zx} & 0 & 0 & 0 \\ -\alpha_{xy} & \alpha_{xy}+\alpha_{yz} & -\alpha_{yz} & 0 & 0 & 0 \\ -\alpha_{zx} & -\alpha_{yz} & \alpha_{yz}+\alpha_{zx} & 0 & 0 & 0 \\ - & - & - & - & - & - \\ 0 & 0 & 0 & 6\eta_{xy} & 0 & 0 \\ 0 & 0 & 0 & 0 & 6\eta_{yz} & 0 \\ 0 & 0 & 0 & 0 & 0 & 6\eta_{zx} \end{bmatrix}. \tag{17}$$

For positive $\alpha_{k\ell}$, $\eta_{k\ell}$ matrix $\mathbf{P}$ has the same rank as its isotropic equivalent Eq. (12), which is recovered when all constants are set equal to one. The constraint introduced by normality among strain rates is still the incompressibility condition Eq. (13).

A procedure constructing a matrix $\boldsymbol{\Theta}$ consistent with Eq. (10) is now established. Note first that, since matrices $\mathbf{P}$ and $\mathbf{P}^{\mathrm{I}}$ are *equivalent* (i.e., they have the same dimensions and the same rank) there exists a non-singular matrix $\mathbf{A}$ such that

$$\mathbf{P} = \mathbf{A}^{\mathrm{t}}\mathbf{P}^{\mathrm{I}}\mathbf{A}. \tag{18}$$

Then the matrix

$$\boldsymbol{\Theta} = \mathbf{A}^{-1}\boldsymbol{\Theta}^{\mathrm{I}}\mathbf{A}^{-\mathrm{t}} \tag{19}$$

is associated to $\mathbf{P}$ through Eq. (10). In fact, on the basis of Eqs. (18) and (19) one can write

$$\mathbf{P}\boldsymbol{\Theta}\mathbf{P} = \mathbf{A}^{\mathrm{t}}\mathbf{P}^{\mathrm{I}}\mathbf{A}\mathbf{A}^{-1}\boldsymbol{\Theta}^{\mathrm{I}}\mathbf{A}^{-\mathrm{t}}\mathbf{A}^{\mathrm{t}}\mathbf{P}^{\mathrm{I}}\mathbf{A} = \mathbf{A}^{\mathrm{t}}\mathbf{P}^{\mathrm{I}}\boldsymbol{\Theta}^{\mathrm{I}}\mathbf{P}^{\mathrm{I}}\mathbf{A} = 2\mathbf{A}^{\mathrm{t}}\mathbf{P}^{\mathrm{I}}\mathbf{A} = 2\mathbf{P}. \tag{20}$$

Eq. (19) permits the definition of matrix $\boldsymbol{\Theta}$ if its isotropic equivalent $\boldsymbol{\Theta}^{\mathrm{I}}$ is known. For the case considered, either expression Eq. (14a,b) can be used.

Matrix $\mathbf{A}$ is easily constructed if matrices $\mathbf{P}$ and $\mathbf{P}^{\mathrm{I}}$ are put in canonical (diagonal) form. Since they are both symmetric and positive semidefinite with a single rank deficiency, their eigenvalues, denoted by κ_i and κ_i^{I} respectively ($i = 1, \ldots, 6$), are real and positive except for $\kappa_1 = \kappa_1^{\mathrm{I}} = 0$. The corresponding eigenvectors are also real and can be collected into two orthonormal matrices $\boldsymbol{\Phi}$ and $\boldsymbol{\Phi}^{\mathrm{I}}$. Then one can write

$$\hat{\mathbf{P}} = \mathrm{diag}(\kappa_i) = \boldsymbol{\Phi}^{\mathrm{t}}\mathbf{P}\boldsymbol{\Phi} \qquad \mathbf{P} = \boldsymbol{\Phi}\hat{\mathbf{P}}\boldsymbol{\Phi}^{\mathrm{t}}, \tag{21a, b}$$

$$\hat{\mathbf{P}}^{\mathrm{I}} = \mathrm{diag}\left(\kappa_i^{\mathrm{I}}\right) = \boldsymbol{\Phi}^{\mathrm{I^t}}\mathbf{P}^{\mathrm{I}}\boldsymbol{\Phi}^{\mathrm{I}} \qquad \mathbf{P}^{\mathrm{I}} = \boldsymbol{\Phi}^{\mathrm{I}}\hat{\mathbf{P}}^{\mathrm{I}}\boldsymbol{\Phi}^{\mathrm{I^t}}. \tag{21c, d}$$

If written for the diagonal matrices, the transformation Eq. (18) is, trivially

$$\hat{\mathbf{P}} = \boldsymbol{\Lambda}\hat{\mathbf{P}}^{\mathrm{I}}\boldsymbol{\Lambda} \quad \boldsymbol{\Lambda} = \mathrm{diag}\left(\sqrt{\kappa_i/\kappa_i^{\mathrm{I}}}\right) \qquad \left(\kappa_1/\kappa_1^{\mathrm{I}} = 1\right). \tag{22a, b}$$

Then, Eq. (21a,b) produce the relation

$$\mathbf{P} = \boldsymbol{\Phi}\hat{\mathbf{P}}\boldsymbol{\Phi}^{\mathrm{t}} = \boldsymbol{\Phi}\boldsymbol{\Lambda}\hat{\mathbf{P}}^{\mathrm{I}}\boldsymbol{\Lambda}\boldsymbol{\Phi}^{\mathrm{t}} = \boldsymbol{\Phi}\boldsymbol{\Lambda}\boldsymbol{\Phi}^{\mathrm{I^t}}\mathbf{P}^{\mathrm{I}}\boldsymbol{\Phi}^{\mathrm{I}}\boldsymbol{\Lambda}\boldsymbol{\Phi}. \tag{23}$$

Comparison with Eq. (18) establishes

$$\mathbf{A} = \boldsymbol{\Phi}^{\mathrm{I}}\boldsymbol{\Lambda}\boldsymbol{\Phi}^{\mathrm{t}}. \tag{24}$$

The structure of the matrices involved makes computations very simple. In fact, by partitioning them into 3×3 blocks, one writes

$$\mathbf{P}^{\mathrm{I}} = \begin{bmatrix} \mathbf{p}^{\mathrm{I}} & \mathbf{0} \\ \mathbf{0} & 6\mathbf{I}_3 \end{bmatrix} \quad \mathbf{P} = \begin{bmatrix} \mathbf{p} & \mathbf{0} \\ \mathbf{0} & \mathrm{diag}(6\eta_{k\ell}) \end{bmatrix}. \tag{25a, b}$$

The block diagonal nature of both matrices and the fact that their lower diagonal blocks are themselves diagonal establish that matrix $\mathbf{A}$ has the form

$$\mathbf{A} = \begin{bmatrix} \mathbf{a} & \mathbf{0} \\ \mathbf{0} & \mathbf{b} \end{bmatrix} \quad \text{with } \mathbf{b} = \begin{bmatrix} \sqrt{\eta_{xy}} & 0 & 0 \\ 0 & \sqrt{\eta_{yz}} & 0 \\ 0 & 0 & \sqrt{\eta_{zx}} \end{bmatrix} \tag{26a, b}$$

and only the 3×3 matrix $\mathbf{a}$ needs to be computed. To this purpose, eigenvalues and eigenvectors of matrix $\mathbf{p}^{\mathrm{I}}$ are evaluated. One obtains

$$\kappa_1^{\mathrm{I}} = 0, \quad \boldsymbol{\phi}_1^{\mathrm{I}} = \frac{1}{\sqrt{3}} \begin{Bmatrix} 1 \\ 1 \\ 1 \end{Bmatrix}, \qquad \kappa_2^{\mathrm{I}} = \kappa_3^{\mathrm{I}} = 3, \quad \boldsymbol{\phi}_{2,3}^{\mathrm{I}} = \frac{1}{\sqrt{2a^2+6b^2}} \begin{Bmatrix} b+a \\ b-a \\ -2b \end{Bmatrix} \tag{27a, b}$$

where a and b can be arbitrarily chosen, provided that the two eigenvectors in Eq. (27b) are mutually orthogonal. The same computation on $\mathbf{p}$ establishes that Eq. (27a) defines the first eigenvalue and eigenvector for this matrix also. The remaining eigenvalues κ_2 and κ_3 must be computed as functions of the values assumed by the coefficients $\alpha_{k\ell}$ for the material considered and, in general, will be different from each other. The corresponding eigenvectors, even when uniquely defined, are still expressed by Eq. (27b) written for the particular values of a and b dictated by the solution of the eigenvalue problem. In other words, the eigenvectors of $\mathbf{p}$ are also eigenvectors of $\mathbf{p}^{\mathrm{I}}$ and the choice $\boldsymbol{\Phi}^{\mathrm{I}} = \boldsymbol{\Phi}$ is legitimate.

Let lower case symbols denote quantities referring to the upper diagonal blocks of the matrices Eq. (25a,b). For the orthonormal transformation matrix and for the matrix Eq. (22b) one writes, respectively

$$\boldsymbol{\varphi} = \boldsymbol{\varphi}^{\mathrm{I}} = [\,\boldsymbol{\phi}_1 \quad \boldsymbol{\phi}_2 \quad \boldsymbol{\phi}_3\,] \quad \boldsymbol{\lambda} = \begin{bmatrix} 1 & 0 & 0 \\ 0 & \sqrt{\kappa_2/3} & 0 \\ 0 & 0 & \sqrt{\kappa_3/3} \end{bmatrix}. \tag{28a, b}$$

On this basis, the expression of matrix $\mathbf{a}$ becomes

$$\mathbf{a} = \boldsymbol{\varphi}\boldsymbol{\lambda}\boldsymbol{\varphi}^{\mathrm{t}} = \mathbf{a}^{\mathrm{t}}. \tag{29}$$

This matrix is straightforwardly inverted. Matrix φ being orthonormal ($\boldsymbol{\varphi}^{-1} = \boldsymbol{\varphi}^{\mathrm{t}}$), the result reads

$$\mathbf{a}^{-1} = \boldsymbol{\varphi}\boldsymbol{\lambda}^{-1}\boldsymbol{\varphi}^{\mathrm{t}} = \mathbf{a}^{-\mathrm{t}}. \tag{30}$$

Account taken of Eq. (26a,b), the expression Eq. (19) of matrix $\boldsymbol{\Theta}$ becomes

$$\boldsymbol{\Theta} = \begin{bmatrix} \mathbf{a}^{-1}\boldsymbol{\vartheta}^{\mathrm{I}}\mathbf{a}^{-1} & \mathbf{0} \\ \mathbf{0} & \mathrm{diag}(1/3\eta_{k\ell}) \end{bmatrix}. \tag{31}$$

$\boldsymbol{\vartheta}^{\mathrm{I}}$ is the 3×3 upper diagonal block of matrix $\boldsymbol{\Theta}^{\mathrm{I}}$, depending on which of the expressions in Eq. (14a,b) is selected. The lower diagonal block is independent of this choice.

The definition of matrix $\boldsymbol{\Theta}$ merely requires the computation of the two non-trivial eigenvalues of $\mathbf{p}$ and of the corresponding eigenvectors. A general expression is not difficult to obtain, but cumbersome to write. The procedure is now illustrated for some particular cases.

3.1. Transversally isotropic behavior

Consider a material isotropic in the plane $z = 0$. Let

$$\bar{\sigma}_x = \bar{\sigma}_y = \sigma_0 \quad \bar{\tau}_{xy} = \frac{1}{\sqrt{3}}\sigma_0 \quad \bar{\sigma}_z = \frac{1}{\beta}\sigma_0 \quad \bar{\tau}_{zx} = \bar{\tau}_{zy} = \frac{1}{\mu}\sigma_0. \tag{32}$$

Then, the coefficients in Eq. (16a,b) are

$$\alpha_{xy} = 2 - \beta^2 \quad \alpha_{yz} = \alpha_{zx} = \beta^2 \quad \eta_{xy} = 1 \quad \eta_{yz} = \eta_{zx} = \frac{\mu^2}{3}. \tag{33}$$

Matrix **P**, Eq. (17), can now be defined. In particular, its upper diagonal block **p** reads

$$\mathbf{p} = \begin{bmatrix} 2 & -(2-\beta^2) & -\beta^2 \\ -(2-\beta^2) & 2 & -\beta^2 \\ -\beta^2 & -\beta^2 & 2\beta^2 \end{bmatrix}. \tag{34}$$

Convexity requires $0 \leqslant \beta \leqslant 2$. The matrix has rank two if both limits are complied with as strict inequalities. Its two non-trivial eigenvalues and eigenvectors are

$$\kappa_2 = 3\beta^2, \quad \boldsymbol{\phi}_2 = \frac{1}{\sqrt{6}}\begin{Bmatrix} 1 \\ 1 \\ -2 \end{Bmatrix} \qquad \kappa_3 = 4 - \beta^2, \quad \boldsymbol{\phi}_3 = \frac{1}{\sqrt{2}}\begin{Bmatrix} 1 \\ -1 \\ 0 \end{Bmatrix}. \tag{35}$$

Account taken of Eq. (27a), Eq. (28a,b) provide

$$\boldsymbol{\varphi} = \begin{bmatrix} \frac{1}{\sqrt{3}} & \frac{1}{\sqrt{6}} & \frac{1}{\sqrt{2}} \\ \frac{1}{\sqrt{3}} & \frac{1}{\sqrt{6}} & -\frac{1}{\sqrt{2}} \\ \frac{1}{\sqrt{3}} & -\frac{2}{\sqrt{6}} & 0 \end{bmatrix} \quad \boldsymbol{\lambda} = \begin{bmatrix} 1 & 0 & 0 \\ 0 & \beta & 0 \\ 0 & 0 & \sqrt{\frac{4-\beta^2}{3}} \end{bmatrix}. \tag{36a, b}$$

Matrix $\mathbf{a}^{-1}$ is readily computed from Eq. (30) and, on this basis, the expression Eq. (31) for $\boldsymbol{\Theta}$ is obtained. It reads

$$\boldsymbol{\Theta} = \begin{bmatrix} \boldsymbol{\vartheta} & \mathbf{0} \\ \mathbf{0} & \boldsymbol{\vartheta}_* \end{bmatrix} \quad \text{with } \boldsymbol{\vartheta}_* = \begin{bmatrix} 1/\mu^2 & 0 & 0 \\ 0 & 1/\mu^2 & 0 \\ 0 & 0 & 1/3 \end{bmatrix} \tag{37a, b}$$

and $\boldsymbol{\vartheta}$ given by one of the following alternatives:

$$\boldsymbol{\vartheta}_1 = \frac{2}{9\beta^2}\begin{bmatrix} \frac{2+4\beta^2}{4-\beta^2} & \frac{2-5\beta^2}{4-\beta^2} & -1 \\ \frac{2-5\beta^2}{4-\beta^2} & \frac{2+4\beta^2}{4-\beta^2} & -1 \\ -1 & -1 & 2 \end{bmatrix} \qquad \boldsymbol{\vartheta}_2 = \frac{2}{9\beta^2}\begin{bmatrix} \frac{2+8\beta^2-\beta^4}{4-\beta^2} & \frac{2-\beta^2-\beta^4}{4-\beta^2} & \beta^2-1 \\ \frac{2-\beta^2-\beta^4}{4-\beta^2} & \frac{2+8\beta^2-\beta^4}{4-\beta^2} & \beta^2-1 \\ \beta^2-1 & \beta^2-1 & \beta^2+2 \end{bmatrix}. \tag{38a, b}$$

Eq. (38a) assumes $\boldsymbol{\Theta}^{\mathrm{I}} = \boldsymbol{\Theta}^{\mathrm{I}}_1$, Eq. (14a). If Eq. (14b) is used instead ($\boldsymbol{\Theta}^{\mathrm{I}} = \boldsymbol{\Theta}^{\mathrm{I}}_2$), Eq. (38b) is obtained. The quadratic forms associated to the two matrices are different, but their values coincide when the incompressibility constraint is introduced. In fact, by eliminating, e.g., $\dot{\varepsilon}_z = -\dot{\varepsilon}_x - \dot{\varepsilon}_y$ one obtains, in both cases

$$\dot{\lambda} = \frac{2}{\beta\sqrt{4-\beta^2}}\sqrt{\dot{\varepsilon}_x^2 + (2-\beta^2)\dot{\varepsilon}_x\dot{\varepsilon}_y + \dot{\varepsilon}_y^2 + \text{shear dissipation}}. \tag{39}$$

3.2. Plane strain

Consider a plane strain state in the plane $z = 0$. Strain rates are now constrained by the conditions $\dot{\varepsilon}_z = \dot{\gamma}_{zx} = \dot{\gamma}_{zy} = 0$, which imply, through the normality rule Eq. (2) and account taken of Eq. (17)

$$\frac{\partial f}{\partial \sigma_z} = -\alpha_{zx}\sigma_x - \alpha_{yz}\sigma_y + \left(\alpha_{yz} + \alpha_{zx}\right)\sigma_z = 0, \tag{40a}$$

$$\frac{\partial f}{\partial \tau_{yz}} = 6\eta_{yz}\tau_{yz} = 0 \qquad \frac{\partial f}{\partial \tau_{zx}} = 6\eta_{zx}\tau_{zx} = 0. \tag{40b, c}$$

Hence, any stress state associated to plane strain flow complies with the conditions

$$\sigma_z = \frac{\alpha_{zx}\sigma_x + \alpha_{yz}\sigma_y}{\alpha_{yz} + \alpha_{zx}} \qquad \tau_{yz} = \tau_{zx} = 0. \tag{41}$$

The relations above can be used to reduce the problem to the strain plane. If they are introduced in the expression Eq. (15) of the yield function, one obtains

$$\varphi = \frac{1}{\sqrt{2}}\sqrt{\alpha\left(\sigma_x - \sigma_y\right)^2 + 6\eta\tau_{xy}^2} - \sigma_0 \leqslant 0, \tag{42}$$

where

$$\alpha = \frac{\alpha_{xy}\alpha_{yz} + \alpha_{yz}\alpha_{zx} + \alpha_{zx}\alpha_{xy}}{\alpha_{yz} + \alpha_{zx}} \tag{43}$$

and η is to be intended as η_{xy}. Matrix $\mathbf{P}$ now reads

$$\mathbf{P} = \begin{bmatrix} \alpha & -\alpha & 0 \\ -\alpha & \alpha & 0 \\ - & - & - \\ 0 & 0 & 6\eta \end{bmatrix}. \tag{44}$$

The matrix above is positive semidefinite with rank two if $\alpha > 0$ and $\eta > 0$. Isotropy is recovered for $\alpha = 3/2$ and $\eta = 1$. In this case, one has

$$\mathbf{P}^{\mathrm{I}} = \frac{3}{2}\begin{bmatrix} 1 & -1 & 0 \\ -1 & 1 & 0 \\ - & - & - \\ 0 & 0 & 4 \end{bmatrix} \qquad \Theta^{\mathrm{I}} = \frac{1}{3}\begin{bmatrix} 1 & -1 & 0 \\ -1 & 1 & 0 \\ - & - & - \\ 0 & 0 & 1 \end{bmatrix}, \tag{45a, b}$$

consistency with Eq. (10) can be verified.

Matrices were partitioned in the spirit of Eq. (25). The upper diagonal block $\mathbf{p}$ is now 2×2 and has the single non-vanishing eigenvalue $\kappa_2 = 2\alpha$. Straightforward computations permit the expressions of the matrices Eq. (28a,b). On this basis, Eqs. (30) and (31) and (45b) provide

$$\mathbf{a}^{-1} = \frac{1}{2}\begin{bmatrix} 1 + \sqrt{\frac{3}{2\alpha}} & 1 - \sqrt{\frac{3}{2\alpha}} \\ 1 - \sqrt{\frac{3}{2\alpha}} & 1 + \sqrt{\frac{3}{2\alpha}} \end{bmatrix} \quad \Theta = \begin{bmatrix} \frac{1}{2\alpha} & -\frac{1}{2\alpha} & 0 \\ -\frac{1}{2\alpha} & \frac{1}{2\alpha} & 0 \\ - & - & - \\ 0 & 0 & \frac{1}{3\eta} \end{bmatrix}. \tag{46a, b}$$

From Eq. (9) it follows:

$$\dot{\lambda} = \sqrt{\frac{1}{2\alpha}(\dot{\varepsilon}_x - \dot{\varepsilon}_y)^2 + \frac{1}{3\eta}\dot{\gamma}_{xy}^2} \tag{47}$$

subject to the incompressibility constraint, which now imposes $\dot{\varepsilon}_x + \dot{\varepsilon}_y = 0$.

Note that the effects of the material coefficients $\alpha_{k\ell}$ are subsumed by the value of α, Eq. (43), so that different materials may give rise to the same plane strain behavior. In particular, the plane strain yield function is not altered when the yield limits in the x and y directions are interchanged.

3.3. Plane stress

Also in this case $\mathbf{P}$ is a 3×3 matrix. Its expression is obtained from Eq. (17) by deleting rows and columns referring to vanishing stress components. If the stress plane is $z = 0$, one obtains

$$\mathbf{P} = \begin{bmatrix} \alpha_{zx} + \alpha_{xy} & -\alpha_{xy} & 0 \\ -\alpha_{xy} & \alpha_{xy} + \alpha_{yz} & 0 \\ 0 & 0 & 6\eta_{xy} \end{bmatrix}. \tag{48a}$$

The matrix is positive definite when

$$\alpha_{xy}\alpha_{yz} + \alpha_{yz}\alpha_{zx} + \alpha_{zx}\alpha_{xy} > 0 \quad \eta_{xy} > 0. \tag{48b}$$

In this case the expression of $\boldsymbol{\Theta}$ is dictated by Eq. (11) and is easily computed. No constraints among the in-plane components of $\dot{\varepsilon}$ are now present.

The relations above permit the following formulation of the kinematic theorem of limit analysis for Hill's condition:

$$s = \min_{\dot{\varepsilon},\dot{\mathbf{u}}} \int_{\Omega} \sigma_0 \sqrt{\dot{\boldsymbol{\varepsilon}}^{t}\boldsymbol{\Theta}\dot{\boldsymbol{\varepsilon}}}\,\mathrm{d}\mathbf{x}, \tag{49a}$$

$$\text{subject to} \quad \dot{\boldsymbol{\varepsilon}} = \nabla_{\mathrm{S}}\dot{\mathbf{u}} \quad \text{in } \Omega \qquad \dot{\mathbf{u}} = \mathbf{0} \quad \text{on } \partial_{\mathrm{U}}\Omega, \tag{49b}$$

$$\dot{\varepsilon}_x + \dot{\varepsilon}_y + \dot{\varepsilon}_z = 0 \quad \text{in } \Omega \qquad \Pi(\dot{\mathbf{u}}) = 1. \tag{49c, d}$$

With respect to Eq. (4a–b), use was made of Eqs. (6) and (9) to express the dissipation power and the condition Eq. (4c) was explicitly written as incompressibility constraint, applying for the plane strain case as well, with $\dot{\varepsilon}_z = 0$.

The structure of Eq. (49a–d) is the same as for the isotropic, von Mises' case and the same techniques can be employed for their solution. A number of methods, based on different strategies and exhibiting different accuracy and computational efficiency, have been proposed in recent years and can be used without modifications. Their description and the assessment of their comparative merits are outside the purpose of this paper, but all of them benefit to a greater or lesser degree from the availability of an explicit expression for the dissipation power.

4. Plane strain examples

Some examples, referring to plane strain situations, are presented to illustrate the influence of orthotropy on the collapse modalities. A simple case, easily solved in closed form, is first considered. It refers to a thick tube (internal radius a, external radius b) subject to uniform internal pressure p. The problem is conveniently formulated in polar coordinates (r, ϑ, z), $z = 0$ being the strain plane. Polar symmetry is preserved if the orthotropy directions coincide with the coordinate axes. Let

$$\bar{\sigma}_r = \frac{\sigma_0}{\beta_r} \quad \bar{\sigma}_\vartheta = \frac{\sigma_0}{\beta_\vartheta} \quad \bar{\sigma}_z = \frac{\sigma_0}{\beta_z} \tag{50}$$

denote the principal uniaxial yield limits. Then, Eqs. (16a) and (43) establish

$$\alpha = \frac{2\beta_r^2\beta_\vartheta^2 + 2\beta_\vartheta^2\beta_z^2 + 2\beta_z^2\beta_r^2 - \beta_r^4 - \beta_\vartheta^4 - \beta_z^4}{2\beta_z^2} \tag{51}$$

and the convexity condition $\alpha > 0$ requires $(\beta_r - \beta_\vartheta)^2 < \beta_z^2 < (\beta_r + \beta_\vartheta)^2$. To make the result independent of the tube thickness, the basic value of the pressure is defined as

$$p = \sigma_0 \ln\left(\frac{b}{a}\right). \tag{52}$$

The only mechanism consistent with the plane strain, axisymmetric nature of the problem and with the incompressibility constraint is governed by radial velocity distribution

$$\dot{s}_r = \frac{a}{r}\dot{u} \tag{53a}$$

$\dot{u}$ being the value at the inner radius. It follows, for the non-vanishing strain rate components

$$\dot{\varepsilon}_r = \frac{\mathrm{d}\dot{s}_r}{\mathrm{d}r} = -\frac{a}{r^2}\dot{u} \quad \dot{\varepsilon}_\vartheta = \frac{\dot{s}_r}{r} = \frac{a}{r^2}\dot{u}. \tag{53b}$$

Hence

$$\hat{D} = \sigma_0\dot{\lambda} = \frac{\sigma_0}{\sqrt{2\alpha}}\sqrt{(\dot{\varepsilon}_r - \dot{\varepsilon}_\vartheta)^2} = \sigma_0\sqrt{\frac{2}{\alpha}}\frac{a}{r^2}\dot{u}, \tag{54}$$

$$D(\dot{u}) = \int_0^{2\pi}\int_a^b \hat{D} r\,\mathrm{d}r\,\mathrm{d}\vartheta = \sqrt{\frac{2}{\alpha}} 2\pi a\sigma_0 \ln\left(\frac{b}{a}\right)\dot{u}. \tag{55a}$$

Eq. (55a) defines the *objective function* of the problem Eqs. (49a–d) as function of the single free parameter $\dot{u}$. However, no minimization is required, the value of $\dot{u}$ being dictated by Eq. (49d), fixing the mechanism amplitude. Taking account of Eq. (52), this reads

$$\Pi(\dot{u}) = 2\pi a\sigma_0 \ln\left(\frac{b}{a}\right)\dot{u} = 1. \tag{55b}$$

By eliminating $\dot{u}$ from Eqs. (55a) and (55b), one obtains

$$s = \sqrt{\frac{2}{\alpha}}. \tag{56}$$

Without lack of generality, it can be assumed $\beta_r = 1.0$. Then, the convexity condition reads $(1 - \beta_\vartheta)^2 < \beta_z^2 < (1 + \beta_\vartheta)^2$ and, for any given β_ϑ, confines the allowable values of β_z in a rather narrow interval. When either limit is approached, $\alpha \to 0$ and the collapse multiplier grows unbounded.

Results for some values of β_ϑ are plotted in Fig. 1. $\beta_\vartheta = 1.0$ corresponds to isotropic behavior in the plane. For $\beta_\vartheta \geqslant 1.0$ the minimum value of the collapse multiplier is attained for $\beta_z^2 = \beta_\vartheta^2 - 1$ and is $s_{\min} = 1.0$, 15% below the isotropic value. For $\beta_\vartheta \leqslant 1.0$ one has $s_{\min} = 1/\beta_\vartheta$. Since the orthotropy axes in the strain plane may be reversed, the results apply also if the values of β_r and β_ϑ are interchanged.

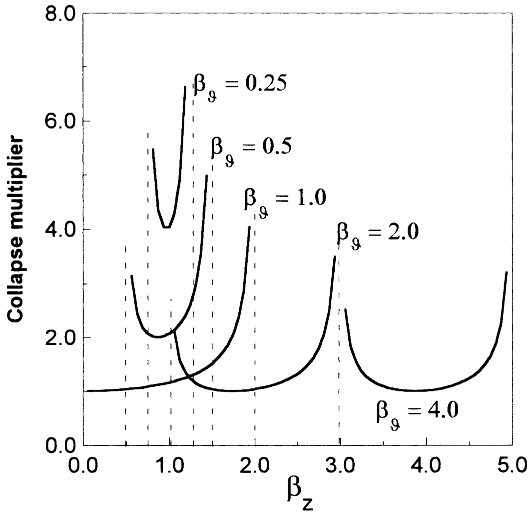

Fig. 1. Collapse multipliers for the plane strain, axisymmetric tube ($\beta_r = 1.0$).

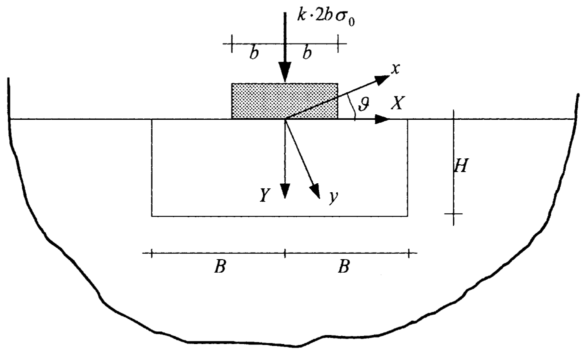

Fig. 2. The punch problem.

The plane strain *punch* problem, originally investigated by Prandtl (1920), is next considered (Fig. 2). The exact collapse multiplier is known in the isotropic case and is $s = 2.969$ if σ_0 (the *uniaxial* yield limit for the material) is assumed as basic load intensity. Numerical solutions are computed by means of the procedure proposed in Capsoni and Corradi (1997) for the von Mises' case, which applies without modifications (for the sake of completeness, an outline of the method and some comments are given in Appendix A). Four node, bilinear elements are employed. Regular subdivisions into square, equal elements are used, with no attempts at designing meshes so as to adapt to predictable mechanisms. This is a deliberate choice, since isoparametrically distorted elements can also be handled (Capsoni, 1999).

As yield limits, the following equivalent alternatives are considered:

$$\bar{\sigma}_y = \sigma_0 \quad \bar{\sigma}_x = \bar{\sigma}_z = \frac{1}{\beta}\sigma_0 \quad \bar{\tau}_{xy} = \frac{1}{\sqrt{3}\eta}\sigma_0, \tag{57a}$$

$$\bar{\sigma}_x = \sigma_0 \quad \bar{\sigma}_y = \bar{\sigma}_z = \frac{1}{\beta}\sigma_0 \quad \bar{\tau}_{xy} = \frac{1}{\sqrt{3}\eta}\sigma_0. \tag{57b}$$

In both instances, Eq. (43) produces

$$\alpha = \frac{4\beta^2 - 1}{2\beta^2}, \tag{58}$$

$\alpha > 0$ requires $\beta > 0.5$.

The situation in which the coordinate axes (X, Y) in the figure coincide with the orthotropy axes (x, y) is first examined. For comparison, a statically admissible (lower bound) multiplier is computed by assuming an equilibrium solution consisting of compression σ_y in a column beneath the load, superimposed to uniform compression σ_x throughout. The plane strain yield condition Eq. (42) is everywhere satisfied for $\sigma_y = -2\sigma_0\sqrt{2/\alpha}$ (where present), $\sigma_x = -\sigma_0\sqrt{2/\alpha}$ and $\tau_{xy} = 0$. The first of these values defines a load intensity that can be safely applied and the corresponding lower bound multiplier is

$$\psi = -\frac{\sigma_y}{\sigma_0} = 2\sqrt{\frac{2}{\alpha}} = \frac{4\beta}{\sqrt{4\beta^2 - 1}} \leqslant s. \tag{59}$$

The lower bound grows without limit for $\beta \to 0.5\,(\alpha \to 0)$, when Eq. (42) becomes independent of normal stresses and any compression can be present beneath the load. On the other hand, when $\beta \to \infty$ Eq. (59) predicts $\psi = 2.0$: even if two of the principal uniaxial yield limits vanish, a finite load can be sustained.

Because of symmetry, only half of the solid is analyzed. A rectangular region of width $B = 6b$ and height $H = 3b$ (Fig. 2) is discretized with 288 finite elements, with side equal to $0.25b$, one quarter of the dimension of the loaded portion. This mesh is large enough to ensure that plastic flow at collapse does not reach the fixed boundary and in the isotropic case produces a collapse multiplier 1.9% in excess of the correct value. Results for different β in the allowable range and some η are listed in Table 1 and illustrated in Fig. 3, together with the lower bound Eq. (59). The increase in load carrying capacity with respect to ψ is mainly due to the presence of shear stresses, ignored by the lower bound. In fact, differences get smaller with increasing η (diminishing yield shear limit). A few computations performed with $\eta = 20$ (black dots in Fig. 3) show that the lower bound, always complied with, is approached even further.

The case in which the orthotropy axes are rotated by an angle ϑ, positive if counterclockwise, with respect to the global reference system (Fig. 2) is next examined. The strain rate components in the two systems are related by the equation

$$\begin{Bmatrix} \dot{\varepsilon}_x \\ \dot{\varepsilon}_y \\ \dot{\gamma}_{xy} \end{Bmatrix} = \begin{bmatrix} \cos^2\vartheta & \sin^2\vartheta & -\sin\vartheta\cos\vartheta \\ \sin^2\vartheta & \cos^2\vartheta & \sin\vartheta\cos\vartheta \\ 2\sin\vartheta\cos\vartheta & -2\sin\vartheta\cos\vartheta & \cos^2\vartheta - \sin^2\vartheta \end{bmatrix} \begin{Bmatrix} \dot{\varepsilon}_X \\ \dot{\varepsilon}_Y \\ \dot{\gamma}_{XY} \end{Bmatrix} \quad \text{or } \dot{\boldsymbol{\varepsilon}}_x = \mathbf{T}\dot{\boldsymbol{\varepsilon}}_X \tag{60}$$

Table 1
Collapse multipliers for the orthotropic punch problem

β	η					ψ
	0.25	0.5	1.0	2.0	4.0	
0.525	7.805		7.003		6.706	6.558
0.6	5.172	4.593	4.215	3.977	3.828	3.618
0.7	4.520		3.517		3.097	2.857
0.8	4.272		3.250		2.815	2.562
0.9	4.142		3.110		2.666	2.405
1.0	4.063	3.442	3.025	2.751	2.576	2.309
1.2	3.973		2.928		2.473	2.200
1.4	3.924		2.876		2.417	2.141
1.6	3.895		2.845		2.383	2.105
1.8	3.876		2.824		2.362	2.082
2.0	3.862	3.235	2.809	2.528	2.346	2.066
∞	3.809		2.752		2.285	2.000

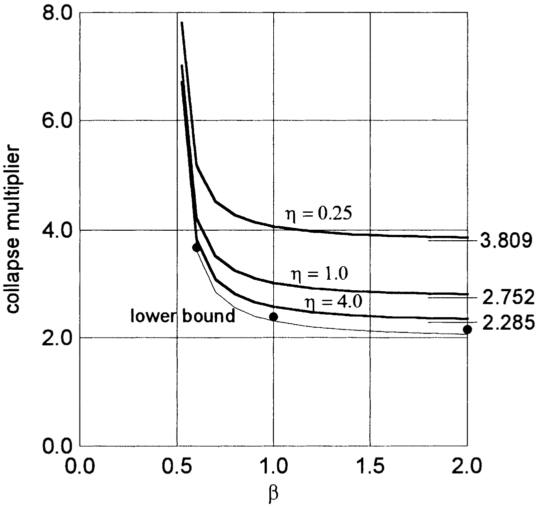

Fig. 3. Collapse multipliers for the orthotropic punch problem ($\vartheta = 0$).

(lower case indices refer to the material principal reference system and capital ones to global coordinates). The expression Eq. (9) of $\dot{\lambda}$ can be written in either form

$$\dot{\lambda} = \sqrt{\dot{\boldsymbol{\varepsilon}}_x^{\mathrm{t}} \boldsymbol{\Theta}_x \dot{\boldsymbol{\varepsilon}}_x} = \sqrt{\dot{\boldsymbol{\varepsilon}}_X^{\mathrm{t}} \boldsymbol{\Theta}_X \dot{\boldsymbol{\varepsilon}}_X}, \tag{61}$$

where for plane strain problems $\boldsymbol{\Theta}_x$ is the matrix Eq. (46b) and, as Eq. (60) establish, $\boldsymbol{\Theta}_X = \mathbf{T}^{\mathrm{t}} \boldsymbol{\Theta}_x \mathbf{T}$. In the case considered, it is convenient to express the angle between the two frames as $\vartheta = \pi/4 \mp \phi$. Then, matrix $\boldsymbol{\Theta}_X$ reads

$$\boldsymbol{\Theta}_X = \begin{bmatrix} \Theta_1 & -\Theta_1 & -\Theta_2 \\ -\Theta_1 & \Theta_1 & \Theta_2 \\ -\Theta_2 & \Theta_2 & \Theta_3 \end{bmatrix} \quad \begin{cases} \Theta_1 = \frac{1}{2\alpha} \sin^2 2\phi + \frac{1}{3\eta} \cos^2 2\phi \\ \Theta_2 = \pm\left(\frac{1}{2\alpha} - \frac{1}{3\eta}\right) \sin 2\phi \cos 2\phi \\ \Theta_3 = \frac{1}{2\alpha} \cos^2 2\phi + \frac{1}{3\eta} \sin^2 2\phi \end{cases}. \tag{62}$$

Observe that a change in the sign in front of ϕ has only the effect of reversing the sign of Θ_2, the coefficient coupling direct and shear strain rates in the expression of $\dot{\lambda}$: as a consequence, the two situations lead to the same collapse multiplier and the collapse mechanism is simply reversed about the Y-axis. To assess the influence of ϑ, only the range $0 \leqslant \vartheta \leqslant \pi/4$ needs to be explored.

Now symmetry cannot be exploited and a rectangle of dimensions $2B \times H$ has to be considered (Fig. 2). Values of B and H larger than in the previous case are assumed, since plastic flow at collapse may spread farther apart on either side ($2B = 20b$ and $H = 4b$ is required to make the collapse mechanism unaffected by the fixed boundary for all ϑ). Due to the increase in the problem dimensions, a coarser mesh was employed, involving 320 elements with side equal to $0.5b$. In this way, the isotropic collapse multiplier is overestimated by about 4%.

Results for $\beta = 2.0$ ($\alpha = 1.875$) and some values of η are plotted in Fig. 4. The case $\eta = 1.0$ shows little dependence from ϑ, because the ratio $2\alpha/3\eta$ is close to one, the value making matrix $\boldsymbol{\Theta}_X$ independent of ϕ and the plane strain behavior indistinguishable from that of a material that exhibits in-plane isotropy. As η departs from unity, differences become significant. Fig. 5, referring to $\eta = 0.25$, shows the collapse mechanisms predicted for some values of ϑ (dashed elements correspond to regions which do not contribute

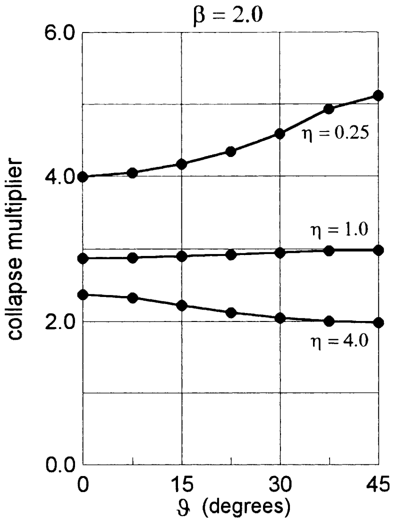

Fig. 4. Collapse multipliers for the punch problem as functions of the inclination of the orthotropy axes.

to plastic flow at collapse). Because of the equivalence of the two assumptions Eqs. (57a) and (57b), for $\vartheta = 45^\circ$ symmetry is recovered.

5. Conclusions

The dissipation power of orthotropic rigid-plastic solids governed by Hill's condition was explicitly expressed in terms of strain rates. On this basis, the kinematic theorem of limit analysis is cast in the same form as for the isotropic, von Mises' case and a number of algorithms developed and successfully tested in the isotropic context can be used for computing the limit load. Some plane strain examples demonstrate the validity of the formulation.

Hill's criterion is a comparatively simple modification of the isotropic von Mises' condition and was probably intended for materials that exhibit relatively small anisotropy, such as cold worked metals. In fact, the requirement that the stress domain be convex imposes rather severe restraints on the ratios between the yield limits in the orthotropy directions, so that the criterion cannot be considered as adequate for several materials of interest, such as fiber reinforced composites. In addition, it was observed that for solids in plane strain normal to an orthotropy axis, the yield limits along the two principal directions in the plane might be interchanged without affecting the result, a property in a sense surprising. This is a consequence of the incompressible nature of plastic flow, but it is not difficult to conceive that it might prove unrealistic in several situations.

The second drawback can be overcome simply by modifying the expression of matrix $\mathbf{P}$, without altering the structure Eq. (1a,b) of the yield function. Actually, removing incompressibility would in general give rise to positive definite matrices and the relevant expressions for $\boldsymbol{\Theta}$ could be obtained directly from Eq. (11). However, this would have little effect on the first limitation and more refined yield functions, such as those based on tensor polynomials of different order (Tsai and Wu, 1971) might be required to model anisotropic yielding with acceptable accuracy. In particular, tensile to compressive strength differentials could be included by supplementing Eq. (1b) with a linear term, and the general expression of the dissipation power in this context is presently searched. This, in turn, will open the way toward the representation of yield

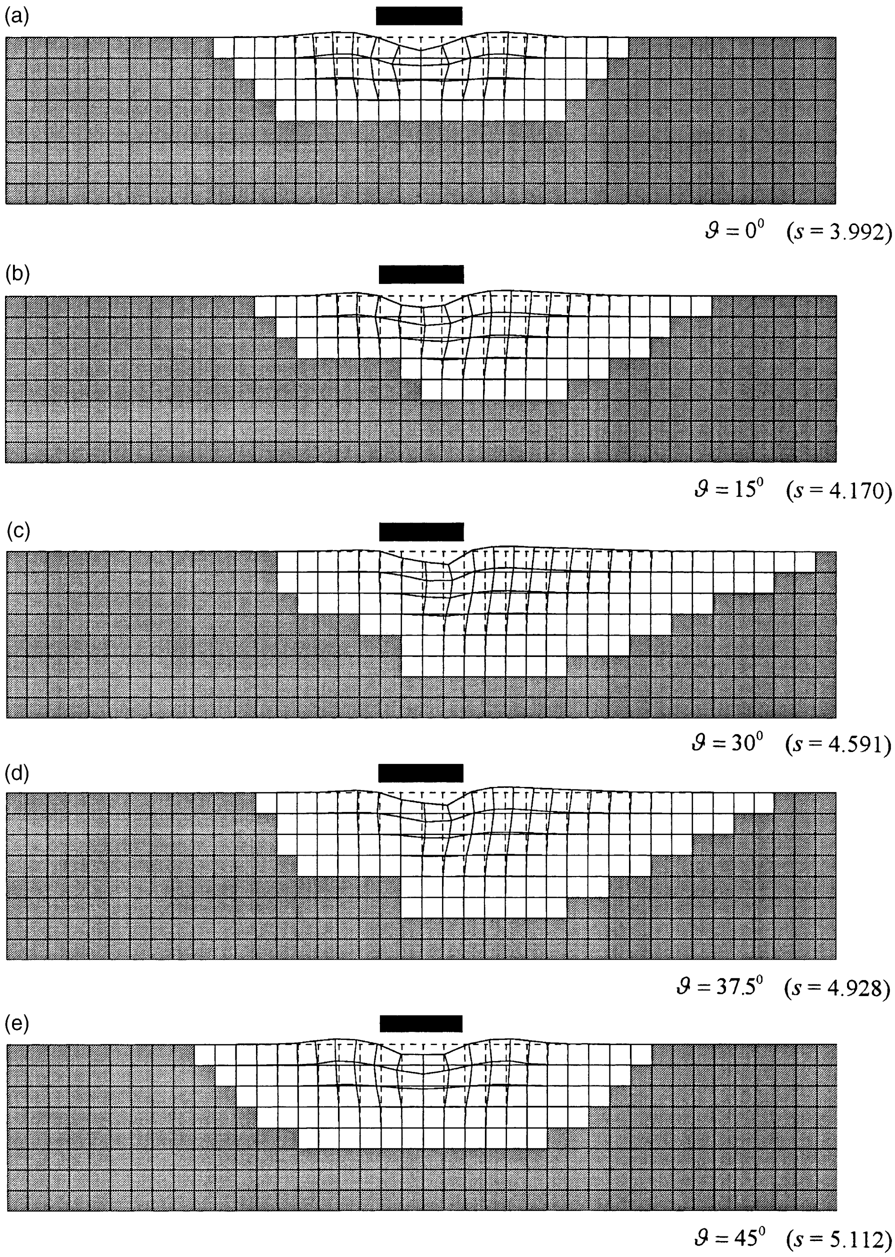

Fig. 5. Collapse mechanisms for the orthotropic punch problem ($\beta = 2.0$, $\eta = 0.25$). Dashed elements do not contribute to plastic flow at collapse. (a) $\vartheta = 0°$ ($s = 3.992$), (b) $\vartheta = 15°$ ($s = 4.170$), (c) $\vartheta = 30°$ ($s = 4.591$), (d) $\vartheta = 37.5°$ ($s = 4.928$) and (e) $\vartheta = 45°$ ($s = 5.112$).

conditions such as anisotropic versions of Mohr–Coulomb's criterion, with plastically admissible strain rate spaces inherently defined by inequalities.

It is worth observing that the explicit expression of the dissipation power is demanded by some solution strategies, directly undertaking the minimization of Eq. (49a) (e.g., Liu et al., 1995; Jiang, 1995; Capsoni and Corradi, 1997), but is not a must for all solution methods. Ponter and Carter (1997) solve a sequence of non-homogeneous elastic problems with material properties adjusted locally so as to recover the power dissipated at collapse as a fictitious elastic energy. The method proposed by Christiansen and Andersen (1999), probably the most effective available at present, considers as practicable a saddle point formulation computing the dissipation power by means of Hill's principle Eq. (5). Nevertheless, it is felt that any method would benefit to some extent from an explicit expression and the present contribution is intended as a starting step in this direction.

Acknowledgements

This work was supported by the Italian Ministry for University and Scientific and Technological Research (MURST).

Appendix A. Outline of the solution procedure and comments

The expression of the dissipation power for Hill's condition can be incorporated advantageously in most solution algorithms and the one employed for solving the punch example by no means is mandatory. Nevertheless, its use is likely to raise some curiosity and a summary of the main steps and some comments are in order. The interested reader is addressed to the original paper (Capsoni and Corradi, 1997) for details.

A discrete form of the problem Eqs. (49a–d) is obtained by standard finite element techniques. In each element e $(e = 1, \dots, N)$ velocities and consequent strain rates are expressed as

$$\dot{\mathbf{u}}_e = \mathbf{N}_e(\mathbf{x})\dot{\mathbf{U}} \qquad \dot{\boldsymbol{\varepsilon}}_e(\mathbf{x}) = \mathbf{B}_e(\mathbf{x})\dot{\mathbf{U}} \quad (e = 1, \dots, N), \tag{A.1a, b}$$

where $\mathbf{N}_e(\mathbf{x})$ is the shape function matrix, from which $\mathbf{B}_e(\mathbf{x})$ follows. $\dot{\mathbf{U}}$ is the vector of the *free* parameters, i.e. assemblage is understood and enforces both interelement continuity and displacement boundary conditions.

At the element level, rigid body motions can be separated from straining modes and Eq. (A.1b) replaced with the two relations (Argyris, 1966)

$$\dot{\boldsymbol{\varepsilon}}_e(\mathbf{x}) = \mathbf{b}_e(\mathbf{x})\dot{\mathbf{q}}_e \quad \dot{\mathbf{q}}_e = \mathbf{C}_e\dot{\mathbf{U}}, \tag{A.2a, b}$$

where $\dot{\mathbf{q}}_e$ is the vector of generalized (or *natural*) strain rates and $\mathbf{C}_e$ are constant matrices, playing the role of compatibility operators for the finite elements.

The splitting above facilitates the elimination of *locking*, an inherent feature of incompressible problems. By using the *enhanced strain* concept (Simo and Rifai, 1990) matrix $\mathbf{b}_e$, as dictated by the displacement approximation, is replaced in Eq. (A.2a) with an expression that makes strain modes other than constant unaffected by the incompressibility constraint, so that the resulting element is locking-free. This amounts at relaxing internal compatibility, but the kinematic nature of the formulation is not jeopardized and results still can be regarded as upper bounds to the collapse multiplier.

Eq. (A.2a,b) can be used to express the objective function Eq. (49a) in terms of $\dot{\mathbf{U}}$, with compatibility fulfilled in the finite element sense. The incompressibility condition Eq. (49c) applies elementwise and provides N constraints among the components of $\dot{\mathbf{U}}$, which can be expressed in terms of a reduced number of free parameters, collected in vector $\dot{\mathbf{U}}_0$. Symbolically, the relation reads

$$\dot{\mathbf{U}} = \mathbf{G}_0\dot{\mathbf{U}}_0. \tag{A.3}$$

After substitution, the minimum problem is brought to the nearly unconstrained form

$$s = \min_{\dot{\mathbf{U}}_0} \sum_{e=1}^{N} D_e(\dot{\mathbf{U}}_0) \quad \text{subject to } \mathbf{F}^{\mathrm{t}}\mathbf{G}_0\dot{\mathbf{U}}_0 = 1 \tag{A.4}$$

with

$$D_e(\dot{\mathbf{U}}_0) = \int_{\Omega_e} \sigma_0 \sqrt{\dot{\mathbf{U}}_0^{\mathrm{t}} \boldsymbol{\Lambda}_{0e}(\mathbf{x}) \dot{\mathbf{U}}_0}\, \mathrm{d}\mathbf{x} \quad \boldsymbol{\Lambda}_{0e} = \mathbf{G}_0^{\mathrm{t}} \mathbf{C}_e^{\mathrm{t}} \mathbf{b}_e^{\mathrm{t}} \boldsymbol{\Theta}_e \mathbf{b}_e \mathbf{C}_e \mathbf{G}_0 \tag{A.5}$$

and $\mathbf{F}$ denoting the vector of nodal forces equivalent to basic loads. By considering the Lagrangean function of the problem, namely

$$L(\dot{\mathbf{U}}_0; \alpha) = \sum_{e=1}^{N} D_e(\dot{\mathbf{U}}_0) - \alpha(\mathbf{P}^{\mathrm{t}}\mathbf{G}_0\dot{\mathbf{U}}_0 - 1) \tag{A.6a}$$

the optimality conditions read

$$\delta L \geqslant 0 \quad \forall \delta\dot{\mathbf{U}}, \delta\alpha. \tag{A.6b}$$

The inequality reflects the non-stationary nature of the optimal value, due to the fact that L is not differentiable in the regions that do not undergo plastic flow. To this purpose, it must be observed that D_e is a global value, referring to a finite element as a whole. In each element, D_e is either positive and differentiable (when $\dot{\mathbf{q}}_e \neq 0$) or equal to zero and not differentiable (if $\dot{\mathbf{q}}_e = 0$). It follows that the set E of the N finite elements is partitioned into the two subsets E_{p} of the $p \leqslant N$ plastic elements and E_{r} of the N-p rigid ones. This plays a key role in the solution strategy, which is now summarized.

Suppose first that all elements undergo plastic flow, so that differentiability is ensured everywhere and L is stationary at solution. Then, the optimality condition reads

$$\frac{\partial L}{\partial \dot{\mathbf{U}}_0} = \sum_{e=1}^{N} \left(\int_{\Omega_e} \sigma_0 \frac{\boldsymbol{\Lambda}_{0e}(\mathbf{x})}{\sqrt{\dot{\mathbf{U}}_0^{\mathrm{t}} \boldsymbol{\Lambda}_{0e}(\mathbf{x}) \dot{\mathbf{U}}_0}} \mathrm{d}\mathbf{x} \right) \dot{\mathbf{U}} - \alpha \mathbf{G}_0^{\mathrm{t}} \mathbf{F} = 0. \tag{A.7}$$

Eq. (A.7) can be solved by direct iteration through the following steps:

$$\mathbf{H}_j = \sum_{e=1}^{N} \left(\int_{\Omega_e} \sigma_0 \frac{\boldsymbol{\Lambda}_{0e}(\mathbf{x})}{\sqrt{\dot{\mathbf{U}}_{0j}^{\mathrm{t}} \boldsymbol{\Lambda}_{0e}(\mathbf{x}) \dot{\mathbf{U}}_{0j}}} \mathrm{d}\mathbf{x} \right) \tag{A.8a}$$

$$\dot{\mathbf{U}}_* = \mathbf{H}_j^{-1} \mathbf{G}_0^{\mathrm{t}} \mathbf{F}, \quad \alpha_j = \frac{1}{\mathbf{F}^{\mathrm{t}} \mathbf{G}_0 \dot{\mathbf{U}}_*}, \quad \dot{\mathbf{U}}_{0(j+1)} = \alpha_j \dot{\mathbf{U}}_* \tag{A.8b–d}$$

which are repeated up to convergence. To this purpose, note that Eq. (A.8c) provides the current estimate of the Lagrangean multiplier α in Eq. (A.6a). At solution, its value can be shown to be equal to the optimal value of the objective function. This property establishes that convergence is attained when one has, to within a given accuracy

$$\sum_{e=1}^{N} D_e\left(\dot{\mathbf{U}}_{0j}\right) = \alpha_{j+1}. \tag{A.8e}$$

As described, the procedure does not consider that often the collapse mechanism entails plastic flow in some elements only. To account for this occurrence, the procedure is started with a tentative vector $\dot{\mathbf{U}}_0$ defined so as to induce plastic flow in all elements. At each iterative step the dissipation power is computed separately for each element and when it gets smaller than a prescribed tolerance, the relevant element is predicted as rigid in the final mechanism. For that element, generalized strain rates must vanish and only rigid body motions survive. Taking account of Eqs. (Ab) and (A.3), the condition reads

$$\dot{\mathbf{q}}_e = \mathbf{C}_e \mathbf{G}_0 \dot{\mathbf{U}}_0 = \mathbf{0}, \tag{A.9}$$

Eq. (A.9) provides some constraints among the components of $\dot{\mathbf{U}}_0$, which can be replaced by a smaller size vector $\dot{\mathbf{U}}_1$ by writing $\dot{\mathbf{U}}_0 = \mathbf{G}^1 \dot{\mathbf{U}}_1$. The iteration process is continued with the rigid element ignored and the operation is repeated whenever the dissipation power of a new element gets sufficiently small.

The procedure aims at identifying the finite elements which are not involved in the collapse mechanism, gradually transferring them from the set E_p of plastic elements (initially including all elements) to the (initially empty) set E_r of rigid ones. A sequence of systems with a progressively decreasing number of elements and of free nodal parameters is thus considered. Each system consists of plastically deforming elements only, and its dissipation power must be stationary at solution.

An inherent limitation of the procedure is that an element cannot be removed from the rigid set E_r once it has been introduced in it. The structural system is progressively modified by the addition of constraints and, whenever this happens, the collapse multiplier of a different structure is searched. Strictly speaking, solutions should be regarded merely as kinematically admissible values, bounding from above the collapse multiplier of the original system. However, the numerical experience gained so far indicates that no wrong elements enter the rigid set.

The compatibility requirement is also worth a comment. As is well known, certain discontinuities in the velocity field do not destroy the validity of the kinematic theorem (Prager, 1954) and in several instances they are actually present at collapse. The velocity model considered is continuous and the solution only converges toward the optimal *continuous* mechanism. Since allowable discontinuities are the limit of continuous fields, reasonable estimates should be arrived at with increasing mesh refinement. In fact, numerical results for the isotropic punch problem (a severe test from this point of view) show that the actual limit value is slowly but steadily approached (Capsoni, 1999). However, otherwise unnecessarily fine meshes are required and the possibility of including discontinuities would improve performances and is worth exploring. Shear discontinuities between elements were considered (e.g., Sloan and Kleeman, 1995), but this implies that meshes be designed in view of expected mechanisms (intraelement discontinuities, like in fracture mechanics, would overcome the problem). An attractive alternative is automatic mesh refinement, which eventually concentrates a large number of small elements in the discontinuity regions (Christiansen and Pedersen, 1999).

In spite of the limitations above, the procedure proves robust and reliable. The incompressibility constraint is enforced strictly on completely locking-free elements, in contrast to similar approaches (e.g., Liu et al., 1995), which both impose it and remove locking by means of penalty factors, with inherent approximations. The elimination of rigid elements also provides benefit, by removing the regions where numerical trouble induced by lack of differentiability arises, a problem often handled by means of regularization (Jiang, 1995) or by introducing ad hoc devices (Liu et al., 1995). The remarks above are not meant at underrating alternative proposals, producing excellent results, but it is felt that the approach indicated entails some improvement. As an example, in all the situations examined so far (isotropic plates were also studied, Capsoni and Corradi, 1999) the convergence test Eq. (A.8e) was met to eight significant figures. This is far more than required in practice, but it gives a nearly absolute confidence on the reliability of the procedure.

The computational efficiency is hard to assess in general terms, since it strongly depends on the number of rigid elements and on the rapidity at which they are detected, so that the solution times for comparable problems might differ up to a factor of four. As an indication, it is mentioned that the examples presented were run on a P/100 PC and the total time required by each solution ranged from 20 to 50 min. The last figure was cut down to 2 min on a HP Work Station with a 400 MHz CPU speed. Significant saving still can be envisaged, since computational efficiency was not aimed at frantically and programming is far from optimal. At present, more meaningful seems an indication on the number of iterations needed. Each problem required 60–80 of them, referring to a number of degrees of freedom decreasing from 304 (after the enforcement of incompressibility) to final values of 60–75, depending on the number of plastic elements survived. Most of them (about 80%) operate on the nearly final configuration. Roughly, the time spent in eliminating rigid elements is the 50% of the total. In any case, this operation and the additional iterations required when the configuration is updated are more than compensated by the reduction in the problem size. Obviously, comparison with methods designed in view of computational efficiency (e.g., Christiansen and Andersen, 1999) is out of question, but the approach appears capable of solving not only examples but also problems of engineering interest.

As a final remark, it is also mentioned that the formulation is not confined to specific finite elements and any locking-free model is easily included.

References

Argyris, J.H., 1966. Continua and discontinua. Proc. First Conf. on Matrix Methods in Structural Mechanics, AFFDL, TR 66-88, Dayton OH, pp. 11–92.

Belytschko, T., Hodge Jr., Ph.G., 1970. Plane stress limit analysis by finite elements. Proc. ASCE J. Engng. Mech. Div. 96, 931–944.

Bottero, A., Negre, R., Pastor, J., Turgeman, S., 1980. Finite element method and limit analysis theory for soil mechanics problems. Comp. Meth. Appl. Mech. Engng. 22, 131–149.

Capsoni, A., 1999. A mixed finite element model for plane strain limit analysis computations. Commun. Num. Meth. Engng 15, 101–112.

Capsoni, A., Corradi, L., 1997. A finite element formulation of the rigid-plastic limit analysis problem. Int. J. Numer. Meth. Engng 40, 2063–2086.

Capsoni, A., Corradi, L., 1999. Limit analysis of plates – a finite element formulation. Struct. Engng. Mech. 8, 325–341.

Casciaro, R., Cascini, L., 1982. A mixed formulation and mixed finite elements for limit analysis. Int. J. Num. Meth. Engng. 18, 211–243.

Charnes, A., Greenberg, H.J., 1951. Plastic collapse and linear programming. American Mathematical Society, Abstract No. 506.

Christiansen, E., Andersen, K.D., 1999. Computation of collapse states with von Mises type yield condition. Int. J. Num. Meth. Engng. 46, 1185–1202.

Christiansen, E., Pedersen, O.S., 1999. Automatic mesh refinement in limit analysis. Institut for Matematik og Datalogi, SDU, Odense Universitet, Preprint No 19.

Cohn, M.Z., Maier G. (Eds.), 1979. Engineering Plasticity by Mathematical Programming. Pergamon Press, New York.

Hill, R., 1947. A theory of the yielding and plastic flow of anisotropic materials. Proc. Roy. Soc. A193, 281–297.

Hodge Jr., Ph.G., Belytschko, T., 1968. Numerical methods for the limit analysis of plates. Trans. ASME, J. Appl. Mech. 35, 796–802.

Jiang, G.L., 1995. Nonlinear finite element formulation of kinematic limit analysis. Int. J. Num. Meth. Engng. 38, 2775–2807.

Koiter, W.T., 1960. General theorems for elastic–plastic solids. In: Sneddon, I.N., Hill, R. (Eds.), Progress in Solid Mechanics, vol. I. North Holland, Amsterdam, pp. 167–221.

Liu, Y.H., Cen, Z.Z., Xu, B.Y., 1995. A numerical method for plastic limit analysis of 3-D structures. Int. J. Solids Struct. 32, 1645–1658.

Ponter, A.R.S., Carter, K.F., 1997. Limit state solutions based upon linear elastic solutions with a spatially varying elastic modulus. Comp. Meth. Appl. Mech. Engng. 140, 237–258.

Prager, W., 1954. Discontinuous fields of plastic stresses and flow. Proc. Second US Congress on Applied Mechanics. Ann Arbor, Michigan, pp. 21–32.

Prandtl, L., 1920. Ueber die haerte plastischer koerper. Goettinger Nachr Math-Phys. Kl. 12, 74–85.

Simo, J.C., Rifai, M.S., 1990. A class of assumed strain methods and the method of incompatible modes. Int. J. Num. Meth. Engng. 29, 1595–1638.

Sloan, S.W., Kleeman, P.W., 1995. Upper bound limit analysis using discontinuous velocity fields. Comp. Meth. Appl. Mech. Engng. 127, 293–314.

Tsai, S.W., Wu, E.M., 1971. A general theory of strength for anisotropic materials. J. Compos. Mater. 8, 58–80.

Yang, G., 1988. Panpenalty finite element programming for plastic limit analysis. Comput. Struct. 28, 749–755.